ChemComm

Chemical Communications

Accepted Manuscript

Volume 54
Number 1
4 January 2018
Pages 1-112

ChemComm

Chemical Communications

rsc.li/chemcomm

COMMUNICATION
S. J. Connon, M. O. Senge et al.
Conformational control of nonplanar free base porphyrins: towards bifunctional catalysts of tunable basicity

ISSN 1359-7345

ROYAL SOCIETY
OF CHEMISTRY

ROYAL SOCIETY
OF CHEMISTRY

rsc.li/chemcomm

COMMUNICATION

Drug orientations within statin-loaded lipoprotein nanoparticles by ^{19}F solid-state NMR

Sophie Lau,[a] Naomi Stanhope,[a] John Griffin,[a] Eleri Hughes,[a] David A. Middleton*[a]

NMR measurements of ^{19}F chemical shift anisotropy and ^{1}H-^{19}F dipolar couplings provide unprecedented information on the molecular orientations of two fluorine-containing statin drugs within the heterogeneous environment of reconstituted high-density lipoprotein (rHDL) nanoparticles, a drug delivery system under clinical investigation.
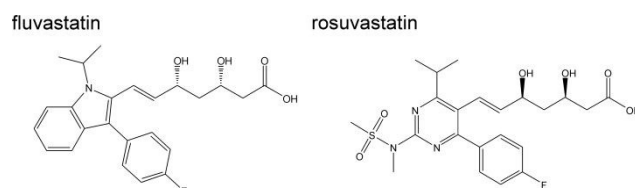
Apolipoprotein A-I; solid-state NMR; drug delivery; HDL

The high cost of bringing a new pharmaceutical to market – an estimated $2.6 billion - reflects the fact that 85-90 % of drug candidates do not progress through clinical trials.[1] One reason for this high attrition rate is the failure of drugs to engage effectively with their molecular target(s) in human patients,[2] and this has motivated efforts to develop smart, nanoscale formulations to lengthen drug circulation times *in vivo*, access impervious tissue and increase the probability of drug-target interactions. Nanoparticle-mediated drug delivery offers the opportunity to rejuvenate clinical failures and repurpose existing drugs, and the US Food and Drug Administration has approved around 60 nanoparticle formulations to date.[3] Correspondingly, as increasingly sophisticated formulations enter development there is a growing need for analytical research tools and quality-control methods to characterise nanoparticles and their cargo at the atomic and molecular levels and to explore the mechanisms of drug delivery.

Here we use ^{19}F NMR as a sensitive probe of the molecular orientations of fluorine-containing drugs as they undergo anisotropic motion within a reconstituted high-density lipoprotein (rHDL) nanoparticle formulation. rHDL nanoparticles are attractive drug delivery vehicles that are well-tolerated *in vivo*, do not invoke an immune response and are capable of delivering lipophilic drugs to tissues via specific receptors.[4, 5] The clinically-tolerated rHDL

preparations CER-001 and CSL112 are nanodiscs comprising a phosphatidylcholine or sphingomyelin/phosphatidylglycerol lipid bilayer surrounded by a helical belt of recombinant apolipoprotein A-I (apoA-I), the 28-kDa major protein component of natural HDL.[6, 7] The position of the native cholesteryl ester (CE) cargo within the core of natural HDL is important for cellular transfer via the SR-B1 receptor,[8] and packaging by the nanodiscs may similarly influence the cellular uptake of drugs. Transfer of CE, vitamins and drugs from HDL into cells is in part mediated by scavenger receptors (e.g., SR-B1), which have channel-forming extracellular domains that selectively bind certain lipophilic molecules and transfer them to the cytoplasm.[9] A drug's orientation within the rHDL lipid matrix will influence how the drug is presented to a receptor and so may affect the rate and selectivity of transfer.[10]

We exploit ^{19}F chemical shifts and ^{1}H-^{19}F dipolar couplings[11] to compare the orientations of two lipophilic fluoroaromatic drugs within the lipid bilayer component of rHDL particles. We chose as our drugs two fluorine-bearing statins, fluvastatin (logP = 4.17) and rosuvastatin (logP = 1.47) (Scheme 1); statin-loaded rHDL nanoparticles have been shown to reduce atherosclerotic lesions in an atherosclerosis mouse model.[12] We prepared nanoparticles of rHDL comprising palmitoyl oleoyl phosphatidylcholine (POPC), fluvastatin or rosuvastatin and full-length apoA-I in a 100:10:1 molar ratio using a detergent-mediated dialysis method. Native gel electrophoresis indicates that the particle size ranges from 8 - 10 nm and transmission electron microscopy (TEM) confirms the characteristic discoidal morphology of the particles (Figure 1A, left and middle). A circular dichroism (CD) spectrum (Figure 1A, right) indicates that apoA-I adopts the expected predominantly (84 %) α-helical conformation. It should be noted that similar-sized truncated apoA-I/lipid nanodiscs are widely used in biological NMR to analyse

a. *Department of Chemistry, Lancaster University, Lancaster LA1 4YB, United Kingdom*

† Footnotes relating to the title and/or authors should appear here.
Electronic Supplementary Information (ESI) available: [Methods and materials, Additional spectra and calculations]. See DOI: 10.1039/x0xx00000x

Scheme 1. Chemical structures of fluorine-containing statins.

COMMUNICATION

the structures of membrane-embedded proteins, as their rapid tumbling times conveniently provide high-resolution spectra.[13] Here the isotropic molecular tumbling of nanodiscs in solution would obscure the effects of local anisotropic motions of the drug that convey information about drug orientation, so we precipitated the nanoparticles from aqueous solution to eliminate particle tumbling. The fluid hydrated lipid bilayer is preserved in the precipitate, as indicated by a ^{31}P NMR spectrum of the POPC phosphate groups with the characteristic 45 ppm width and axially symmetric line shape (Figure 1B, left).[14, 15] A ^{15}N magic angle spinning NMR spectrum of precipitated rHDL particles constructed from ^{15}N-labelled apoA-I confirms that protein is also present in the precipitate and the backbone chemical shifts are consistent with the expected predominantly α-helical structure (Figure 1B, right).

Statins embedded in the rHDL lipid bilayer will undergo anisotropic motions that scale the ^{19}F chemical shift anisotropy in a predictable way that depends on the drug's orientation in the planar matrix.[11] Molecules rotate about a principal axis that runs parallel with the bilayer normal and the NMR line shape is sensitive to the orientations of the ^{19}F chemical shift tensor elements δ_{11}, δ_{22} and δ_{33} relative to this axis, as defined by angles α and β (Figure 1C). If the chemical shift tensor orientation relative to the molecular geometry is known, one can relate the measured chemical shift anisotropy to the average orientation of the drug in the lipid bilayer. DFT calculations predict that the ^{19}F chemical shift tensor is oriented with the least-shielded component δ_{11} exactly in plane with the aromatic ring and δ_{22} directed along the fluorine-carbon bond (Figure S1), as seen for other fluorophenyl compounds.[11] Additional random motional fluctuations of the molecule about the two axes perpendicular to the main axis must also be considered in the analysis, as must internal rotations of the fluoroaromatic ring (Figure

1C). Random fluctuations are described by an order parameter, S_{mol}, which describes the maximum angular excursion θ from the principal axis through $S_{mol} = \cos(\theta)$

Proton-decoupled ^{19}F NMR spectra confirm that the two statins are present in the rHDL formulations (fluvastatin in Figure 2A and rosuvastatin Figure S2A). Whereas the ^{19}F chemical shift anisotropy Δδ of the two statins in the solid state is ~60 ppm, with an asymmetry parameter η of ~0.7 (Figure S1 and Table S1), the spectra of the rHDL formulations indicate an approximate 10-fold reduction in the observed anisotropy and an apparent axially symmetric chemical shift tensor (η = 0) (Table S2). These features confirm that the molecules undergo anisotropic rotation and give a scaled chemical shift anisotropy, $\Delta\delta_{av}$, of 6.2 ppm for fluvastatin and 8.3 ppm for rosuvastatin. The absence of narrow peaks at the isotropic chemical shifts of the statins indicates that the drugs are not distributed between the nanoparticles and the residual aqueous phase but are confined within the lipid matrix. Calculations of the expected value of $\Delta\delta_{av}$ for different values of α and β (varying each from 0° to 180°) reveal that the maximum possible value of $\Delta\delta_{av}$ is 4.6 ppm for fluvastatin and 4.9 ppm for rosuvastatin (Figure S2B) when rotation of the fluorophenyl ring is considered in addition to the overall molecular rotation. These $\Delta\delta_{av}$ values are smaller than the observed values and hence free rotation of the fluorophenyl ring must be slow on the NMR (μs) time scale, possibly because of a high energy barrier resulting from steric clashes between the aromatic and heptenoic acid protons.
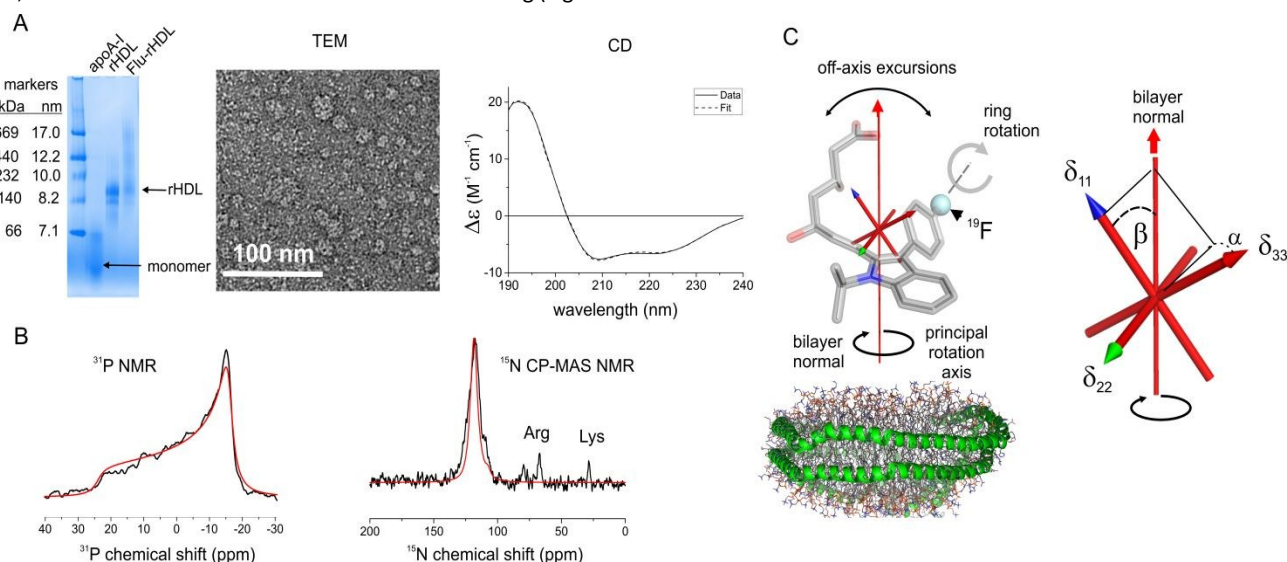

Figure 1. Encapsulation of statins within rHDL particles. A: Native gel electrophoresis (left) and TEM (middle) confirm the presence of rHDL particles approximately 8 - 10 nm in diameter in the absence or presence of fluvastatin. CD spectroscopy (right) indicates the presence of predominantly helical protein. B: ^{31}P NMR (left) confirms the presence of lamellar POPC lipids in PEG precipitated rHDL and ^{15}N CP-MAS NMR (right) indicates that the helical structure of apoA-I is retained in the PEG precipitate. The red line is a simulated line shape comprising the predicted backbone ^{15}N chemical shifts of all residues of apoA-I in a fully helical conformation. C: Rapid dynamics of a statin embedded in a lipid bilayer of rHDL that may scale the ^{19}F chemical shift anisotropy. The principal axes of the ^{19}F chemical shift tensor are shown with the origin at the centre of mass of the molecule. Angles α and β define the ^{19}F principal axes relative to the principal rotation axis, which is parallel with the bilayer normal, and the axis of the aromatic ring rotation is parallel with the direction of ^{19}F chemical shift tensor component δ_{22}. Off-axis excursions are represented by an order parameter $S_{mol} = \cos(\theta)$.
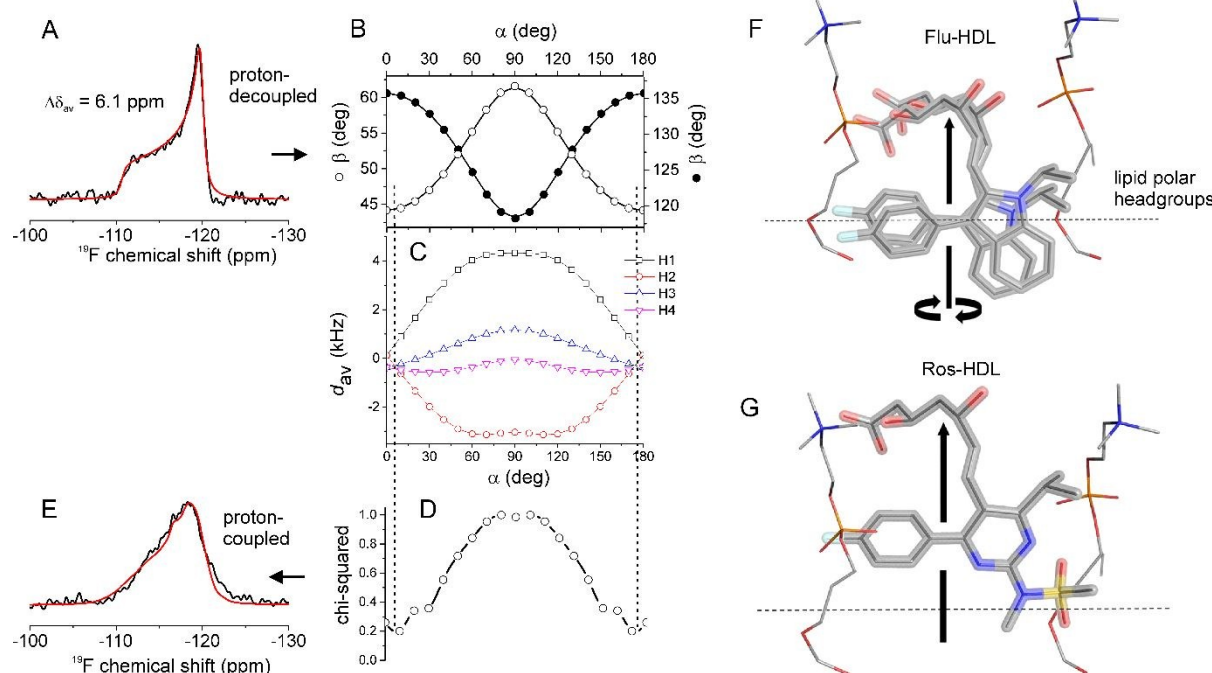
Figure 2. The average orientations of statins with the lipid bilayers of rHDL particles from ^{19}F NMR lineshape analysis. A: Spectrum of fluvastatin in rHDL (black). The value of $\Delta\delta_{av}$ (6.1 ppm) was obtained by least-squares fitting of a simulated lineshape (red). B: The measured $\Delta\delta_{av}$ is consistent with the pairs of α and β values shown by the continuous lines. Discrete values of α (in 5° increments) and corresponding β values (denoted by the filled and open circles, in 10° increments for clarity) were used to simulate proton-coupled spectra as described below. C: Each of the discrete [α, β] pairs define a specific statin orientation relative to a principal axis of rotation. From each orientation the rotationally-averaged dipolar couplings d_{av} between ^{19}F and the 4 protons (H1-H4) in the fluorophenyl ring were calculated. D: Proton-coupled spectra were simulated for each [α, β] pair and the corresponding dipolar coupling values. Chi-squared values represent the agreement between each simulated spectrum and the experimental dipolar-coupled spectrum. E: The line of closest agreement with the proton-coupled spectrum (chi-squared minimum) is consistent with 4 [α, β] values given in Table S3. F: Average orientations of fluvastatin and rosuvastatin in rHDL bilayers. Vertical arrows denote the principal axis of rotation, which is parallel with the bilayer normal.

Figures 2B and S3B show that the $\Delta\delta_{av}$ values measured from the proton-decoupled spectra are consistent with a continuum of α and β values, with α ranging from 0 - 180° and β ranging from 40° - 65°. To restrict further the range of possible molecular orientations defined by these angles, we obtained proton-coupled ^{19}F NMR spectra of the rHDL formulations to obtain line shapes that are modulated by ^{1}H-^{19}F dipolar interactions within the statin fluoroaromatic ring. The magnitude of the dipolar couplings is, like $\Delta\delta_{av}$, sensitive to the orientation of the statins relative to their principal rotation axis. We calculated the dynamically-averaged dipolar coupling constants, d_{av}, for 36 discrete pairs of α and β along the continuum (Figures 2C and S3C). We then simulated a series of proton-coupled ^{19}F NMR line shapes based on the calculated couplings and the measured $\Delta\delta_{av}$ values for each statin to find the values of α and β achieving the closest agreement with the experimental line shapes according to chi-square analysis (Figures 2D and S3-S5). For fluvastatin, the closest agreement is obtained with four [α, β] combinations and for rosuvastatin with two [α, β] combinations (Table S3, Figures 2E and S2E). Discrepancies between the simulated and experimental spectra may reflect minor contributions from longer-range inter- and intramolecular couplings, which could not be included in the simulations. For each pair of angles, errors of ±5° in α and ±1.5° in β reflect the uncertainty in S_{mol}, the true value of which we

assume lies between the extremes of 0.5 (θ = 60°) and 1.0 (θ = 0°). The value of S_{mol} reported for sterol molecules is ~0.8.[16, 17]

After taking into consideration the out-of-plane fluorophenyl ring conformation of the two statins, as determined from crystal structures and by energy minimisation (Figure S6) we translated the angles into two possible mean
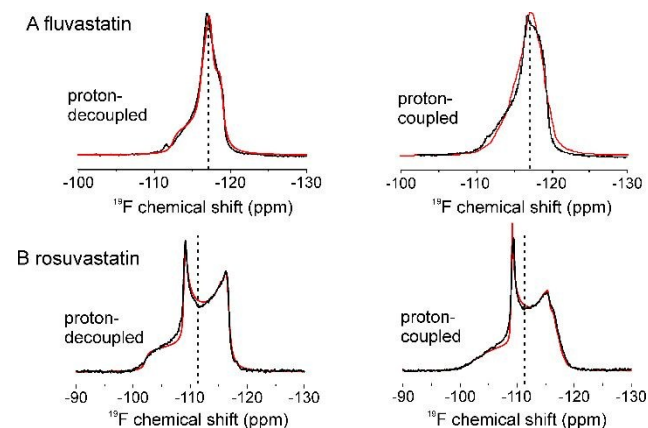

Figure 3. Proton-decoupled and proton-coupled ^{19}F NMR spectra of fluvastatin (A) and rosuvastatin (B) embedded in POPC MLVs. Experimental spectra (black) are overlaid with best-fitting simulated-two component lineshapes (red). The two values of $\Delta\delta_{av}$ obtained from the two components of each spectrum are given in Table S2 and the values of α and β calculated from the spectra are given in Table S3. Dotted lines indicate the isotropic chemical shifts.

COMMUNICATION

orientations of fluvastatin about its principal axis of rotation in the lipid bilayer (Figure 2F, top) and one orientation of rosuvastatin (Figure 2F, bottom), as well as their mirror images. The two molecules adopt similar orientations in the lipid matrix. Solution-state ^{1}H-^{1}H NOESY NMR spectra of fluvastatin in dodecylphosphocholine micelles revealed cross peaks between the aromatic protons of the drug and headgroup and hydrocarbon chain protons of the lipid, suggesting that the aromatic ring serves as a hydrophobic anchor and the dihydroxyheptenoic acid is associated with the lipid headgroups.[18, 19] Here, a NOESY NMR spectrum of fluvastatin in POPC multilamellar vesicles (MLVs), obtained with magic-angle spinning, revealed cross peaks between protons in the fluoroaromatic ring and hydrocarbon chain protons (Figure S7), confirming that the ring serves as a hydrophobic anchor. This may explain the restricted rotation of the ring.

Lastly, we asked whether the statins adopt similar orientations in spherical, protein-free POPC MLVs. In contrast to the rHDL spectra, the ^{19}F proton-decoupled and coupled spectra of the MLVs (Figure 3) each comprise two components in approximately equal proportion. The narrow component in the spectra of rosuvastatin (Figure 3B) does not arise from an isotropic population of the drug (i.e., that is rapidly tumbling in solution or smaller vesicles) because the component is offset from the isotropic chemical shift. All spectra could be simulated by two anisotropic components, one with $\Delta\delta_{av} > 0$ and the other with $\Delta\delta_{av} < 0$ (Table S2), indicating that each statin adopts two different average orientations in the MLV bilayers. The spectra illustrate how highly sensitive this method is to minor alterations in molecular orientation, because analysis of the two spectral components for each statin reveals very close values of α and β for the molecules in each population (Table S3). The sensitivity of the α and β values to orientation also reveal that fluvastatin and rosuvastatin adopt very subtly different orientations in POPC MLVs and in rHDL.

There is still much to learn about the molecular packaging of drugs by nanoparticles, yet these details may influence how drugs transfer to the recipient tissue. Here we have shown an NMR method exploiting chemical shifts and dipolar couplings to determine the mean orientations of drugs within the lipid matrix of rHDL nanoparticles. About 30 % of small molecule drugs contain fluorine [20] and so the ^{19}F NMR method could be applicable to up to 750 approved and 1600 experimental drugs, depending on their suitability for HDL encapsulation. The high sensitivity of the ^{19}F NMR line shape to just minor adjustments of molecular orientation makes it a useful method for structure-activity studies relating the molecular orientations of drugs to the rates of transfer to tissue, and for analysing the reproducibility of formulations.

Conflicts of interest

There are no conflicts to declare.

Notes and References

1. C. H. Wong, K. W. Siah and A. W. Lo, *Biostatistics*, 2019, **20**, 273-286.
2. T. J. Hwang, D. Carpenter, J. C. Lauffenburger, B. Wang, J. M. Franklin and A. S. Kesselheim, *Jama Internal Medicine*, 2016, **176**, 1826-1833.
3. D. Bobo, K. J. Robinson, J. Islam, K. J. Thurecht and S. R. Corrie, *Pharmaceutical Research*, 2016, **33**, 2373-2387.
4. R. Kuai, D. Li, Y. E. Chen, J. J. Moon and A. Schwendeman, *Acs Nano*, 2016, **10**, 3015-3041.
5. A. G. Lacko, N. A. Sabnis, B. Nagarajan and W. J. McConathy, *Frontiers in Pharmacology*, 2015, **6**.
6. S. Diditchenko, A. Gille, I. Pragst, D. Stadler, M. Waelchli, R. Hamilton, A. Leis and S. D. Wright, *Arteriosclerosis Thrombosis and Vascular Biology*, 2013, **33**, 2202-2211.
7. C. H. Keyserling, R. Barbaras, R. Benghozi and J. L. Dasseux, *Clinical Drug Investigation*, 2017, **37**, 483-491.
8. S. T. Thuahnai, S. Lund-Katz, D. L. Williams and M. C. Phillips, *J. Biol. Chem.*, 2001, **276**, 43801-43808.
9. D. Neculai, M. Schwake, M. Ravichandran, F. Zunke and R. F. e. a. Collins, *Nature*, 2013, **504**, 172-176.
10. W. V. Rodrigueza, S. T. Thuahnai, R. E. Temel, S. Lund-Katz, M. C. Phillips and D. L. Williams, *J. Biol. Chem.*, 1999, **274**, 20344-20359.
11. E. Hughes, J. M. Griffin, M. P. Coogan and D. A. Middleton, *Physical Chemistry Chemical Physics*, 2018, **20**, 18207-18215.
12. R. Duivenvoorden, J. Tang, D. P. Cormode, A. J. Mieszawska, D. Izquierdo-Garcia, C. Ozcan, M. J. Otten, N. Zaidi, M. E. Lobatto, S. M. van Rijs, B. Priem, E. L. Kuan, C. Martel, B. Hewing, H. Sager, M. Nahrendorf, G. J. Randolph, E. S. G. Stroes, V. Fuster, E. A. Fisher, Z. A. Fayad and W. J. M. Mulder, *Nature Communications*, 2014, **5**.
13. A. Viegas, T. Viennet and M. Etzkorn, *Biological Chemistry*, 2016, **397**, 1335-1354.
14. E. E. Burnell, P. R. Cullis and B. Dekruijff, *Biochimica Et Biophysica Acta*, 1980, **603**, 63-69.
15. P. M. Macdonald, Q. Saleem, A. Lai and H. H. Morales, *Chemistry and Physics of Lipids*, 2013, **166**, 31-44.
16. N. Matsumori, Y. Kasai, T. Oishi, M. Murata and K. Nomura, *JACS*, 2008, **130**, 4757-4766.
17. O. Soubias, F. Jolibois, S. Massou, A. Milon and V. Reat, *Biophys. J.*, 2005, **89**, 1120-1131.
18. L. F. Galiullina, O. V. Aganova, I. A. Latfullin, G. S. Musabirova, A. V. Aganov and V. V. Klochkov, *BioNanoScience*, 2016, **6**, 352-354.
19. L. F. Galiullina, O. V. Aganova, I. A. Latfullin, G. S. Musabirova, A. V. Aganov and V. V. Klochkov, *Biochem. Biophys. Acta*, 2017, **1859**, 295-300.
20. Y. Zhou, J. Wang, Z. N. Gu, S. N. Wang, W. Zhu, J. L. Acena, V. A. Soloshonok, K. Izawa and H. Liu, *Chem. Rev.*, 2016, **116**, 422-518.